JOURNAL OF AGRICULTURAL AND FOOD CHEMISTRY

Article

pubs.acs.org/JAFC

Characteristics and Essences upon Conjugation of Imidacloprid with Two Model Proteins

Fei Ding,[†,‡] Wei Peng,[§] Jian-Xiong Diao,[⊥] Li Zhang,[§] and Ying Sun*[,⊥]

[†]Department of Chemistry, [§]Key Laboratory of Pesticide Chemistry and Application Technology, Ministry of Agriculture, Department of Applied Chemistry, and [⊥]College of Resources and Environmental Sciences, China Agricultural University, Beijing 100193, China

[‡]Department of Biological Engineering, Massachusetts Institute of Technology, Cambridge, Massachusetts 02139, United States

ABSTRACT: Since the introduction of imidacloprid in the early 1990s, it has become one of the most widely applied insecticides, and currently represents about 20% of the global pesticide market (Tomizawa, M.; Casida, J. E. *J. Agric. Food Chem* **2011**, *59*, 2883−2886). In the context of this study, our major aim was to comprehensively scrutinize the nature of imidacloprid with two typical model proteins, lysozyme and albumin, by means of circular dichroism (CD), steady-state and time-resolved fluorescence, and molecular modeling at the molecular level. Far-UV CD verified that the spatial structure of both proteins was altered with a distinct reduction of α helix in the presence of imidacloprid suggesting unfolding of the protein (i.e., protein damage). The data of steady-state and time-resolved fluorescence showed that the conjugation of imidacloprid with lysozyme yielded quenching by a static mechanism (K_{SV} = 3.841 × 10^4 M^{-1}), while combined static and dynamic properties existed for albumin tryptophan (Trp)-214 fluorescence. Molecular modeling simulations displayed that the imidacloprid binding site was near to the Trp-62 and Trp-63 residues of lysozyme, and it was located at the subdomain IIA (warfarin-azapropazone site) of albumin. Furthermore, the primary forces between protein and imidacloprid are hydrogen bond, hydrophobic, and $\pi-\pi$ interactions, but the affinity of lysozyme with imidacloprid is much lower than albumin, probably because the affinity distinctions stem from discrepancy in the three-dimensional structure of the two globular proteins. The results presented here will help to further understand the credible mechanism by which the toxicological implication of neonicotinoid insecticides is palliated by carrier protein.

KEYWORDS: *neonicotinoid insecticide, imidacloprid, protein, circular dichroism, fluorescence, molecular modeling*

INTRODUCTION

Nowadays, pesticides stand for one of the greatest environmental problems, because as the world population increases, the necessity to enlarge agricultural productivity will pass into inevitable.[1] This fact will lead to an even greater growth of the production and consumption of agrochemical compounds (mainly pesticides). Unfortunately, large-scale public application of various pesticides may bring about the contamination of different environmental matrices such as air, water, soils, animal species, and agricultural products, as a consequence of migration or accumulation of those chemicals or plants that are in contact with these compounds.[2] Imidacloprid, 1-(6-chloro-3-pyridylmethyl)-*N*-nitroimidazolidin-2-ylideneamine (structure shown in Figure 1), the representative of the neonicotinoid insecticides, was patented in 1985 by Bayer CropScience and was launched on the market in 1991.[3] It is a highly effective insecticide for which the mode of action has been found to derive from the almost complete and irreversible blocking of the postsynaptic nicotinergic acetylcholine receptors.[4] Imidacloprid has been registered in approximately 120 countries and is used on over 140 agricultural and horticultural cultivated crops, for example, rice, cereals, maize, potatoes, vegetable, sugar beet, fruit, cotton, hops, and turfs; it therefore accounts for 20% of the total insecticide world market.[5]

The United Nations evaluate that less than 1% of all pesticides used in agriculture actually reach the crops;[6] the residuals are in many cases toxic and nonbiodegradable, and they tend to accumulate in the environment with unpredictable consequences for the midterm future.[7] Imidacloprid has relatively high water solubility (0.51−0.61 g L^{-1} at 20 °C) and the potential to move into surface water and to leach into groundwater, slow degradation (half-life in water is 31−46 days), and the tendency to stay in soil (half-life in soil is 69−997 days).[8,9] Latterly, certain pesticides (including imidaclo-

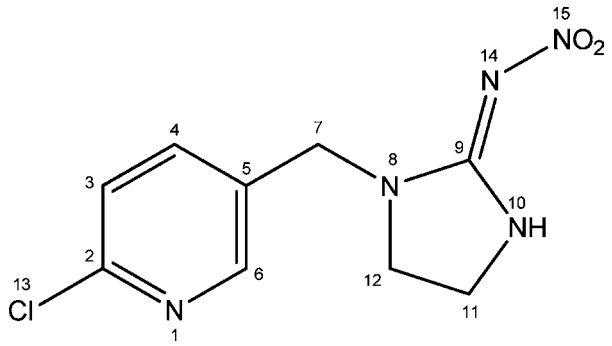

Figure 1. Molecular structure of imidacloprid.

Received: November 22, 2012
Revised: March 24, 2013
Accepted: March 26, 2013
Published: March 26, 2013

prid) have aroused anxiety owing to its probable endocrine disruptor property, which is known to unfavorably injure reproductive competence of males and females. The plausible reason of the fact is endocrine disruptor chemicals imitate the structure of natural hormones existing in the human body, and their disastrous effects are linked with their capacity to meddle with gonadal steroids performance that eventually produces detrimental influences on grownup reproductive system.[10] For example, it is evaluated that 7.4% of the married women in the United States between ages 15 and 44 are infertile.[1] Consequently, in order to guarantee consumer safety and regulate international trade, maximum residue limits for imidacloprid in foodstuffs have been set by several government agencies, for example, the U.S. Environmental Protection Agency, European Commission, and Health Canada's Pest Management Regulatory Agency.[11−13]

In some earlier studies, imidacloprid generally was considered to have low toxicity, both acute and chronic, to mammals and humans, but growing evidence clearly demonstrated that exposure of imidacloprid may be related with the enriched production of dark consequences in animals and particularly humans. For instance, Feng et al.[14] found that genotoxicity, direct DNA strand breakages, and chromosome/genome mutations could be caused by imidacloprid in human peripheral blood lymphocytes in vitro. In another study, a statistically significant augment in sister chromatid exchange frequency originated from treatments male Wistar rat bone marrow polychromatic erythrocyte in vivo with imidacloprid at doses of 300 mg kg^{-1} of body weight.[15] These phenomena were supported in an investigation by Costa et al.,[16] in which a micronucleus test and a single cell gel electrophoresis assay were utilized to display increased DNA damage and chromosomal aberrations in human cells affirming a genotoxic risk created by imidacloprid. Research on animals has also obviously proved that imidacloprid can bring about mutagenicity, carcinogenicity, oxidative stress, developmental immunotoxicity, and inflammation in the central nervous system and liver in nontarget organisms.[2,17−21] Furthermore, a few cases of acute imidacloprid human poisoning and various fatalities have been reported recently.[22−24] Thus, the utilization of imidacloprid in agriculture has undeniable repercussions in the environment and in the quality of farm produces, and it eventually can turn into a serious hazard for human health.

It is commonly approved today that the conjugation of various ligands or small organic molecules to biomacromolecules such as proteins and nucleic acids by noncovalent interactions is fundamental to many biological processes, and this procedure is an essential element that deeply influences their distribution, duration, excretion, and biomolecular function.[25] In this regard, it is of great interest to check the nature of protein−imidacloprid complexation in the blood plasma to obtain a better grasp of toxicological properties of imidacloprid hauling and allocation among organs as well as the excretion rate. We delineate here a detailed work of the complexation of imidacloprid with lysozyme and albumin, owing to these two proteins are the principal model protein responsible for binding endogenous and exogenous ligands, and the three-dimensional structure of lysozyme and albumin has been elucidated by X-ray crystallography earlier.[26,27] Attempts have been made to characterize the optical properties of the protein−imidacloprid complex by employing circular dichroism (CD), steady-state and time-resolved fluorescence, the structural changes of the protein, affinity of imidacloprid, and the binding mechanism tested at 298 K, and these experimental observations were further interpreted on the basis of molecular modeling simulations executed for the protein−imidacloprid complex. The data generated in this job will gain future risky assessments and also help construct a peculiar pesticide biosensor system for the human health to monitor imidacloprid, which is the most widely used insecticide in the world.[28,29]

MATERIALS AND METHODS

Materials. Lysozyme from chicken egg white (L4919, BioUltra, lyophilized powder, ≥98%), albumin from human serum (A8763, lyophilized powder, essentially globulin free, ≥ 99%), and imidacloprid (37894, analytical standard) were purchased from Sigma−Aldrich (St. Louis, MO) and used without further purification, and deionized water was generated by a Milli-Q ultrapure water purification systems from Millipore (Billerica, MA). Tris (0.2 M)−HCl (0.1 M) buffer of pH = 7.4, with an ionic strength 0.1 in the presence of NaCl, except where specified, was used, and the pH was checked with an Orion-350 PerpHecT advanced benchtop pH meter (Thermo Scientific, Waltham, MA). Dilutions of the protein stock solution (10 μM) in Tris−HCl buffer were prepared immediately before use, and the concentration of protein was measured by the method of Lowry et al.[30] All other reagents employed were of analytical grade and received from Sigma−Aldrich.

CD Spectra. Far-UV CD spectra were collected with a Jasco-810 spectropolarimeter (Jasco, Japan) equipped with a microcomputer, and the instrument was calibrated with d-10-camphorsulfonic acid. All the CD spectra were carried out at 298 K with a PFD-425S Peltier temperature controller attached to a water bath with an accuracy of ±0.1 °C. Each spectrum was performed with use of a quartz cuvette of 0.2 cm path length and taken at wavelengths between 200 and 260 nm with 0.1 nm step resolution and averaged over five scans recorded at a speed of 20 nm min^{-1} and a response time of 1 s. All observed CD spectra were baseline subtracted for buffer, and the secondary structure was computed exploiting Jasco standard spectra analysis software package, which calculates the different designations of secondary structures by comparison with CD spectra, determined from distinct proteins for which high-quality X-ray diffraction data are available.[31]

Steady-State Fluorescence. Steady-state fluorescence was registered on a F-4500 spectrofluorimeter (Hitachi, Japan) equipped with 1.0 cm quartz cell and a thermostatic bath. The protein concentration in all the experiments was 1.0 μM, the excitation and emission slit widths were fixed at 5.0 nm, the excitation wavelength was set at 295 nm to selectively excite the Trp residue, and the emission spectra were recorded in the wavelength range 300−450 nm at a scanning speed of 240 nm min^{-1}. Tris−HCl buffer of imidacloprid in corresponding concentrations was subtracted from all measurements.

Time-Resolved Fluorescence. Time-resolved fluorescence was examined with a FL920P spectrometer (Edinburgh, UK), using the time-correlated single photon counting system with a hydrogen flash lamp excitation source, in air-equilibrated solution at an ambient temperature. The excitation wavelength was 295 nm, and the number of counts gathered in the channel of maximum intensity was 4000. The instrument response function (IRF) was gauged exploiting Ludox to scatter light at the excitation wavelength. The data were analyzed with a nonlinear least-squares iterative method utilizing Edinburgh tail fit software, the IRF was deconvoluted from the experimental data, and the resolution limit after deconvolution was 0.2 ns. The value of χ^2 (0.9−1.2), the Durbin−Watson parameter (greater than 1.7), as well as a visual inspection of the residuals were used to evaluate how well the calculated decay fit the data. Average fluorescence lifetime (τ) for multiexponential function fittings were from the following relation:[32]

$$I(t) = \sum_i A_i e^{-t/\tau_i} \quad (1)$$

where τ_i are fluorescence lifetimes and A_i are their relative amplitudes, with i variable from 1 to 3.

Molecular Modeling. Molecular modeling of the protein−imidacloprid complexation was conducted on SGI Fuel Workstation. The crystal structures of lysozyme (entry codes 6LYZ) and albumin (entry codes 1H9Z), determined at a resolution 2.0 and 2.5 Å, respectively, were retrieved from the Brookhaven Protein Data Bank (http://www.rcsb.org/pdb). After being imported in the program Sybyl version 7.3 (http://tripos.com), protein structure was carefully inspected for atom and bond type correctness assignment. Hydrogen atoms were computationally added using the Sybyl Biopolymer and build/edit menus. To avoid negative acid/acid interactions and repulsive steric clashes, added hydrogen atoms were energy minimized with the Powell algorithm with a convergence gradient of 0.5 kcal (mol Å)$^{-1}$ for 1500 cycles; this procedure does not change positions to heavy atoms, and the potential of the three-dimensional structure of the protein was assigned according to the AMBER force field with Kollman all-atom charges. The two-dimensional structure of imidacloprid was downloaded from PubChem (http://pubchem.ncbi.nlm.nih.gov), and the initial structure of the molecule was yielded by Sybyl 7.3. The geometry of imidacloprid was subsequently optimized to minimal energy using the Tripos force field with Gasteiger−Hückel charges, the Surflex-Dock program that employs an automatic flexible docking algorithm was applied to calculate the possible conformation of the ligand that binds to model protein, and the program PyMOL (http://www.pymol.org) was used for visualization of the molecular docking results.

Statistical Analysis. All assays were executed in triplicate; the mean values, standard deviations, and statistical differences were estimated utilizing analysis of variance (ANOVA). The mean values were compared using student's t test, and all statistic data were treated using the OriginPro Software (OriginLab Corporation, Northampton, MA).

THEORY AND CALCULATION

Fluorescence quenching refers to any process that decreases the fluorescence intensity of a sample. A variety of molecular interactions can result in quenching, such as excited-state reactions, molecular rearrangements, energy transfer, ground-state complex formation, and collisional quenching. Fluorescence quenching is described by the well-known Stern−Volmer equation:[32]

$$\frac{F_0}{F} = 1 + k_q\tau_0[Q] = 1 + K_{SV}[Q] \quad (2)$$

In this equation, F_0 and F are the fluorescence intensities in the absence and presence of quencher, respectively, k_q is the bimolecular quenching constant, τ_0 is the lifetime of the fluorophore in the absence of quencher, $[Q]$ is the concentration of quencher, and K_{SV} is the Stern−Volmer quenching constant. Therefore, eq 2 was applied to fit K_{SV} by linear regression of a plot of F_0/F versus $[Q]$.

RESULTS

Far-UV CD Spectra. As we know, the physiological function of a protein is depended on its structure, and binding of a ligand to proteins usually evokes change to their three-dimensional structures, leading to an alteration of human absorption; thereby, the form of the ligand is regarded as pharmacologically or toxicologically active, and its function links fundamental with the protein−ligand affinity.[33] To analyze the structural changes of protein quantitatively, the raw CD spectra of the protein in the absence and presence of imidacloprid were shown in Figure 2, and secondary structure components computed based on CD data were summarized in Table 1. The CD curves exhibited two negative peaks in the far-UV CD region at 208 and 222 nm, characteristic of an α-helical structure of protein. A reasonable explication is that the negative peaks between 208 and 209 nm and between 222 and 223 nm are both contributed by n → π^* transitions for the peptide bond of the α helix.[31] Table 1 displays free lysozyme contains 43.2% α helix, 18.5% β sheet, 15.1% turn, and 23.2% random coil, while free albumin has 54.3% α helix, 9.6% β

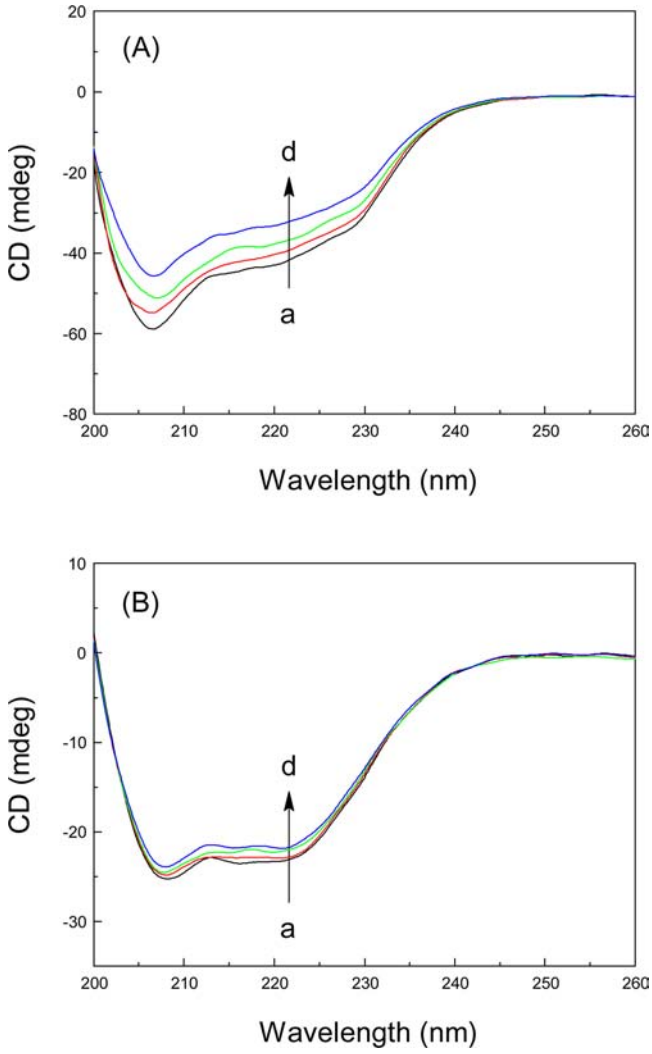

Figure 2. Far-UV CD spectra of (A) lysozyme and (B) albumin complexes with imidacloprid (pH = 7.4, T = 298 K). (a) 1.0 μM protein, (b)→(d) 1.0 μM protein in the presence of 2.0, 4.0, and 8.0 μM imidacloprid.

Table 1. Secondary Structure of Protein Complexes with Imidacloprid at pH 7.4 Assessed by Jasco Standard Spectra Analysis Software

sample	secondary structure components (%)			
	α helix	β sheet	turn	random
free lysozyme	43.2	18.5	15.1	23.2
lysozyme + imidacloprid (1:2)	41.8	18.9	15.7	23.6
lysozyme + imidacloprid (1:4)	38.9	20.1	16.8	24.2
lysozyme + imidacloprid (1:8)	35.6	21.2	17.7	25.5
free albumin	54.3	9.6	12.9	23.2
albumin + imidacloprid (1:2)	52.9	9.9	13.4	23.8
albumin + imidacloprid (1:4)	51.4	10.3	13.9	24.4
albumin + imidacloprid (1:8)	49.3	10.9	14.4	25.4

dx.doi.org/10.1021/jf3048065 | J. Agric. Food Chem. 2013, 61, 4497−4505

sheet, 12.9% turn, and 23.2% random coil; upon complex with imidacloprid, diminution of α helix was noticed from 43.2% free lysozyme to 35.6% (complex) and 54.3% free albumin to 49.3% (complex), while augment in β sheet, turn, and random coil from 18.5%, 15.1%, and 23.2% free lysozyme to 21.2%, 17.7%, and 25.5% (complex) and from 9.6%, 12.9%, and 23.2% free albumin to 10.9%, 14.4%, and 25.4% (complex). The lessening of α helix with an increment in the β sheet, turn, and random coil revealed imidacloprid bound with amino acid residues of the polypeptide chain and caused the destabilization of the model protein spatial structure,[34] that is, some extent of protein unfolding upon imidacloprid binding.

Steady-State Fluorescence. The affinity of protein with imidacloprid was estimated by the measurement of intrinsic fluorescence of Trp residues, and Figure 3 expresses the raw data for quenching of protein fluorescence at pH 7.4 by addition of imidacloprid. It was observed that protein appeared to have a fluorescence peak at 340 nm, following an excitation at 295 nm, and the addition of imidacloprid aroused a gradual reducing of the fluorescence signal. Under the experimental conditions, imidacloprid exhibited no fluorescence emission in the range 300−450 nm, which did not affect protein intrinsic Trp fluorescence. These phenomena illustrated there were reactions between the protein and imidacloprid and imidacloprid was located in the domain where Trp situated within or near the fluorophore.[35] Similar findings have also been depicted by Bourassa and Tajmir-Riahi[36] for the binding of folic acid to milk α- and β-caseins. However, imidacloprid could have different quenching effects and affinities between lysozyme and albumin, which are concerning the three-dimensional structure of these two proteins; this aspect will be further discussed by using molecular modeling in the next section.

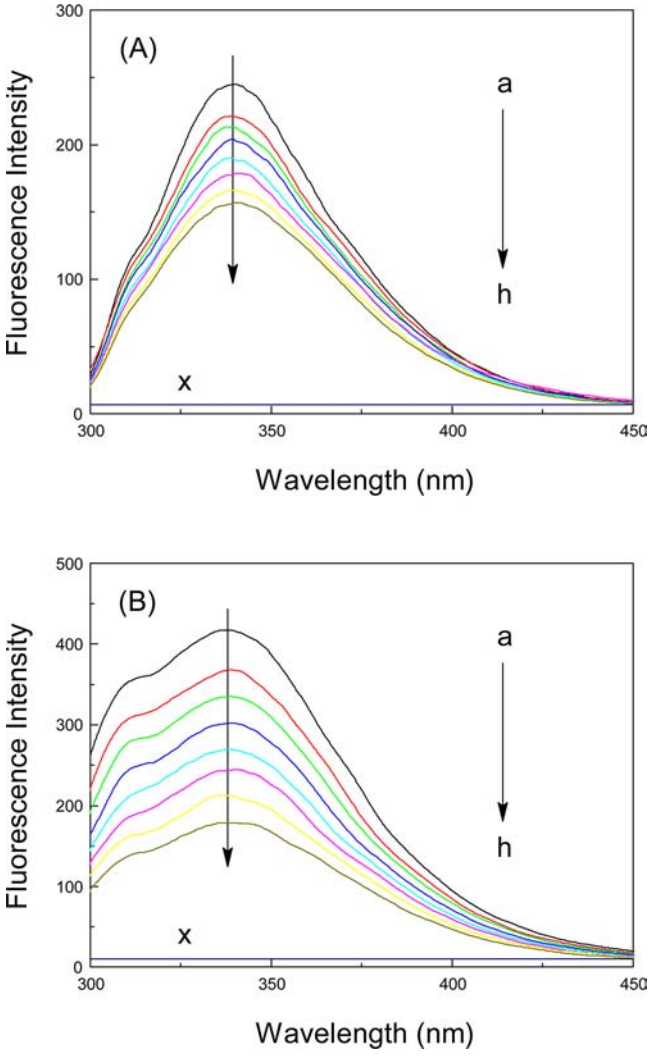

Figure 3. Steady-state fluorescence of (A) lysozyme and (B) albumin with different amounts of imidacloprid (pH = 7.4, T = 298 K). (a) 1.0 μM protein, (b)→(h) 1.0 μM protein in the presence of 2.0, 4.0, 6.0, 8.0, 10, 12, and 14 μM imidacloprid, (x) 14 μM imidacloprid only.

Essence of Protein−Imidacloprid. To explain the nature of fluorescence, the data were fitted according to the Stern−Volmer eq 2; it can plainly be seen from Figure 4, the plot of

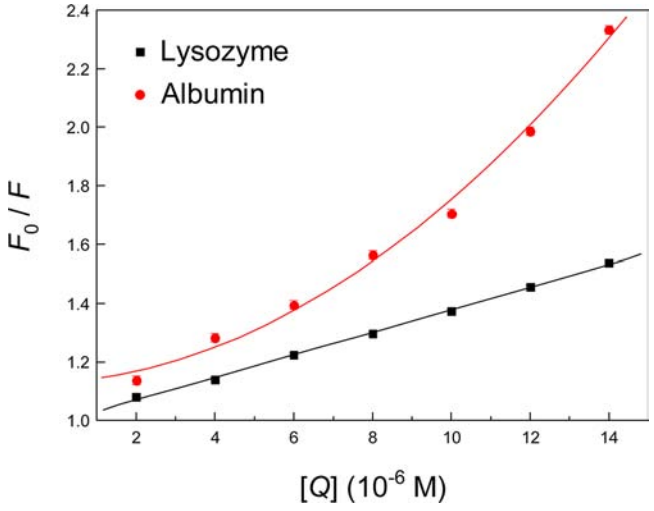

Figure 4. Stern−Volmer plot describing Trp quenching of protein (1.0 μM) at pH = 7.4 in the presence of 2.0, 4.0, 6.0, 8.0, 10, 12, and 14 μM imidacloprid. (■) Lysozyme, $y = 0.03841x + 0.9938$; (▲) albumin, $y = 0.00536x^2 + 0.00896x + 1.129$. Steady-state fluorescence data was collected at λ_{ex} = 295 nm, and the λ_{em} maximum occurred at 340 nm.

F_0/F for lysozyme *against* imidacloprid concentration points to a good linearity (R = 0.9993) and affords K_{SV} and k_q to be 3.841×10^4 M^{-1} and 2.032×10^{13} M^{-1} s^{-1}, respectively. The value of k_q is 3 orders of magnitude greater than the maximum value for diffusion-controlled quenching in water ($\sim 10^{10}$ M^{-1} s^{-1}),[32] so it obviously declares that the fluorescence quenching of lysozyme may be chiefly governed by a static mechanism rather than a dynamic process. But, for the albumin−imidacloprid mixture, the typical feature of Figure 4 in such circumstance is an upward concave toward the y axis, manifesting that the fluorophore in albumin can be quenched both by collisions and by complex formation with imidacloprid, namely, combined dynamic and static quenching.[35] Moreover, static and dynamic quenching can be distinguished by their differing dependence on temperature and viscosity or preferably by fluorescence lifetime measurements. In order to acquire directly proofs of the pith of the protein−imidacloprid association, the representative fluorescence decay profiles of protein at various molar ratios of imidacloprid in Tris−HCl buffer, pH = 7.4, are emerged in Figure 5, and the fluorescence lifetime and their amplitudes are also listed in Table 2. The decay curves fitted well to a biexponential function, and the relative fluorescence lifetimes being begot are τ_1 = 1.58 ns (3.19 ns) and τ_2 = 2.72 ns (7.33 ns) of lysozyme (albumin), while in

dx.doi.org/10.1021/jf3048065 | J. Agric. Food Chem. 2013, 61, 4497−4505

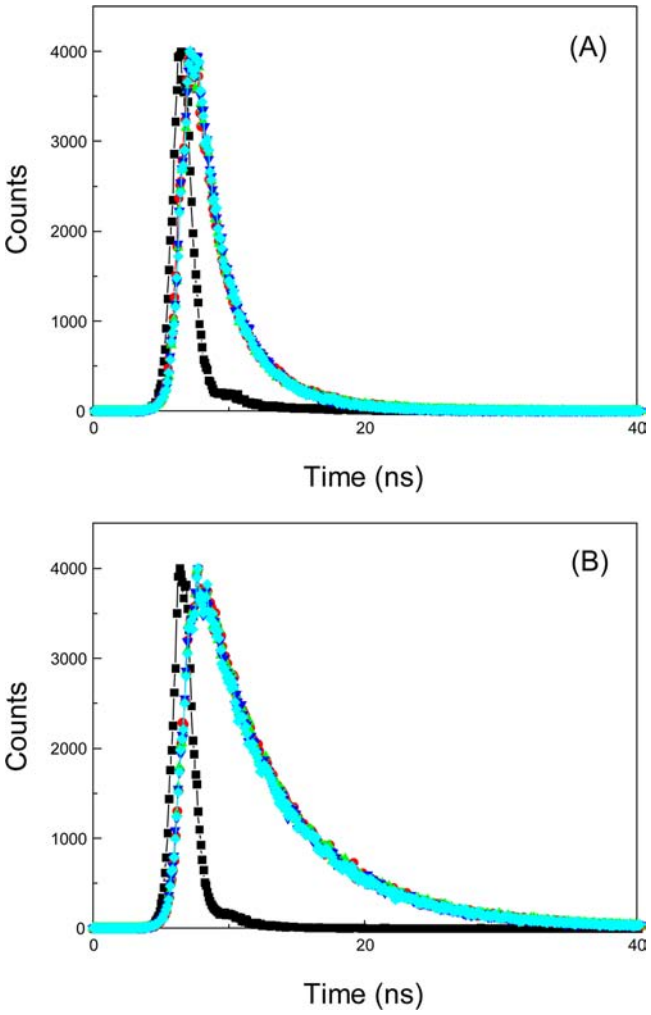

Figure 5. Time-resolved fluorescence decays of (A) lysozyme and (B) albumin in Tris–HCl buffer, pH = 7.4. c(protein) = 10 μM; c(imidacloprid) = 0 (red), 10 (green), 20 (blue), and 40 (cyan) μM. The sharp pattern on the left (black) is the lamp profile.

Table 2. Fluorescence Lifetime of Protein as a Function of Concentrations of Imidacloprid

sample	τ_1 (ns)	τ_2 (ns)	A_1	A_2	τ (ns)	χ^2
free lysozyme	1.58	2.72	0.73	0.27	1.89	1.01
lysozyme + imidacloprid (1:1)	1.23	2.35	0.41	0.59	1.89	1.06
lysozyme + imidacloprid (1:2)	1.13	2.46	0.42	0.58	1.90	1.07
lysozyme + imidacloprid (1:4)	1.09	2.49	0.43	0.57	1.89	1.05
free albumin	3.19	7.33	0.29	0.71	6.13	1.05
albumin + imidacloprid (1:1)	2.99	7.13	0.26	0.74	6.05	1.07
albumin + imidacloprid (1:2)	2.85	7.04	0.27	0.73	5.91	1.06
albumin + imidacloprid (1:4)	2.74	6.92	0.25	0.75	5.88	1.05

the maximum concentration of imidacloprid, the lifetimes are τ_1 = 1.09 ns (2.74 ns) and τ_2 = 2.49 ns (6.92 ns). As Trp is known to show multiexponential decays, we have not tried to designate the individual components, but the average lifetime has been engaged so as to gain a qualitative analysis. The average lifetime of lysozyme did not vary evidently, just from 1.90 to 1.89 ns, at different imidacloprid concentrations, hence signifying quenching is essentially static for lysozyme–imidacloprid.[37] The average fluorescence lifetime decreases from 6.13 to 5.88 ns, stating patently that the quenching of albumin Trp fluorescence by imidacloprid is combined dynamic and static in nature, not simply static quenching. These observations corroborate our foregoing inference grounded on steady-state fluorescence, and we also disagree with the previous outcome of Wang et al.[38]

Molecular Modeling. As mentioned earlier, binding of ligands to protein is exceptionally vital as it can affect the distribution and elimination of the ligand as well as the duration and intensity of its pharmacological and toxicological action; consequently, it is necessary to comprehend the specific binding region of imidacloprid to protein. Molecular modeling simulations were completed to survey the complexation of imidacloprid at the active site of two model proteins, and best energy pictures are shown in Figure 6. As can be seen, the affinity and binding free energies of lysozyme–imidacloprid are 0.6761×10^3 M^{-1} and $\Delta G = -16.14$ kJ mol^{-1}, respectively. The oxygen atom of the nitryl in imidacloprid can make a hydrogen bond (Figure 6A) with the hydrogen atom of the amino group linked to the carbonyl group in Asn-103, and the bond length is 2.88 Å. On the basis of surface modification of imidacloprid and lysozyme, we found that the pyridine ring in imidacloprid is towards the hydrophobic patch that is composed of Ile-58, Trp-62, Trp-63, Ile-98, and Ala-107 residues, attesting hydrophobic interactions operated between them. In addition, the molecular distance between the heart of the pyridine ring in imidacloprid and the benzene ring of Trp-62 and Trp-63 is 3.17 and 5.08 Å, respectively, accordingly proclaiming that π–π interactions also existed between lysozyme and imidacloprid.

For the albumin–imidacloprid system, the affinity and free energies are 1.288×10^4 M^{-1} and $\Delta G = -23.45$ kJ mol^{-1}, respectively. The imidacloprid binding site is situated within subdomain IIA formed by six helices (Figure 6B); the oxygen atom of nitryl, the nitrogen atom N-14, and the hydrogen atom of the secondary amine in the imidazole ring can form hydrogen bonds with the hydrogen atoms of guanidyl in Arg-222 and the oxygen atom of carbonyl group in Ala-291; the bond lengths are 2.42, 1.93, 2.19, and 2.39 Å, respectively. Imidacloprid and subdomain IIA were also surface modified; we can discover a hydrophobic region of subdomain IIA constituted by Phe-211, Trp-214, Ala-215, Leu-238, Val-241, and so forth, and the pyridine ring of imidacloprid is confronted with the patch, which testified that hydrophobic interactions play an important role between them. Likewise, the molecular distance between the center of the pyridine ring in imidacloprid and the core of the benzene ring in Phe-211 and Trp-214 and the imidazole ring in His-242 are 3.5, 3.58, and 4.73 Å, respectively, which enunciated the existence of prominent π–π interactions between albumin and imidacloprid.

DISCUSSION

As previously stated, large-scale populace use of pesticides in public health and agriculture project has engendered catastrophic environmental pollution and health hazards, involving cases of serious acute and chronic human poisoning. Imidacloprid was treated as moderately noxious based on the World Health Organization and categorized by the U.S. Environmental Protection Agency as a toxicity class II/III agent[39,40] because it blocks a specific neuron pathway that is

dx.doi.org/10.1021/jf3048065 | J. Agric. Food Chem. 2013, 61, 4497–4505

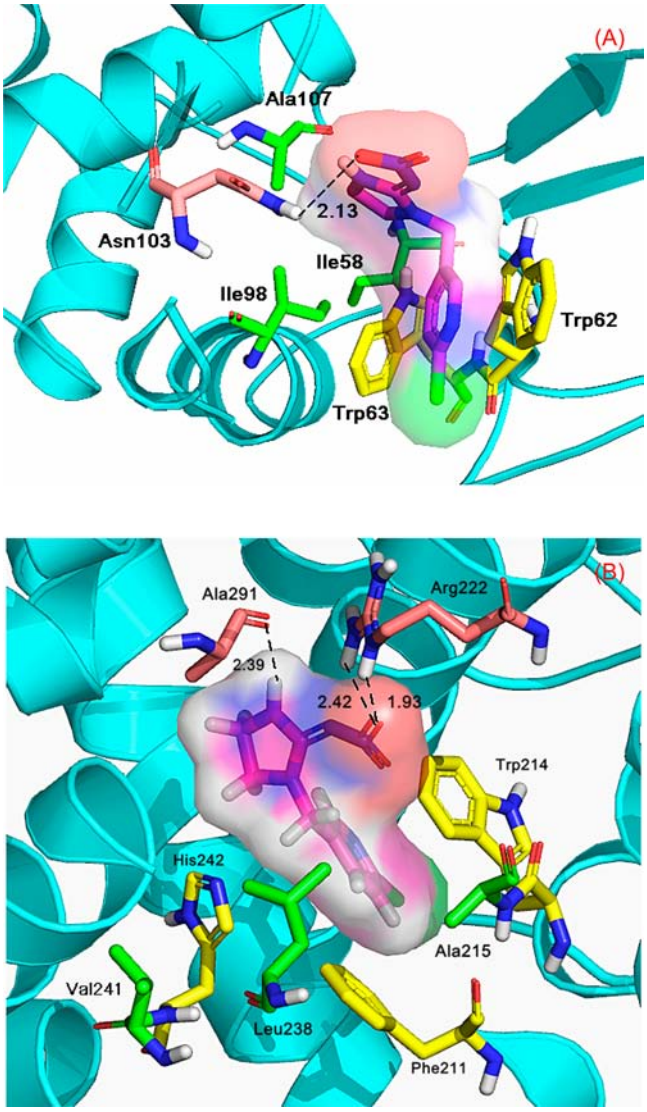

Figure 6. Molecular modeling of imidacloprid docked to (A) lysozyme and (B) albumin. The purple carbon skeleton model shows imidacloprid, colored as per the atoms and possesses translucent surface of electron spin density. The key amino acid residues around imidacloprid have been indicated in the stick model: the pink stick model reveals hydrogen bonds between Asn-103 (A) and Arg-222, Ala-291 (B) residues and imidacloprid; the green stick model illustrates hydrophobic interactions between Ile-58, Trp-62, Trp-63, Ile-98, and Ala-107 (A) and Phe-211, Trp-214, Ala-215, Leu-238, and Val-241 (B) residues and imidacloprid; the yellow stick model expresses $\pi-\pi$ interactions between Trp-62 and Trp-63 (A) and Phe-211, Trp-214, and His-242 (B) residues and imidacloprid. (For interpretation of the references to color in this figure legend, the reader is referred to the web version of the article.)

more bountiful in insects than in warm-blooded animals. Imidacloprid was applied massively as an agrochemical in excess of one decade in North America, since it displaced the frequently used insecticide chlorpyrifos in 2000, and for this reason, its residue is omnipresent; the origins of baring are changed and contain from food chain and water, indoor and outdoor air, household dust, applications to lawns and gardens, and some occupations.[15] On the basis of modern knowledge, almost every ligand appearring in human blood complexes reversibly to plasma proteins, and this noncovalent interaction generates several effects. Protein binding enlarges ligand solubility in plasma, enhancing its shipment to the target tissue, which is exceptionally vital in the case of hydrophobic, low-soluble chemicals.[41] The intensity of conjugation to protein may thus have a sequel for the speed of clearance of metabolites and for their transport to cells and tissues, as described above. Proteins are dynamic molecules whose functions nearly always rely upon complexation with other molecules, and these interactions are influenced in physiologically important ways through generally noticeable changes in protein conformation.[42] Whether such alterations could facilitate or impede the cellular uptake of ligands such as beneficial or poisonous substances is indefinite.

It is apparent that the native conformation of protein and the protein−imidacloprid adduct experience alterations upon imidacloprid complexation in the current work. Diminishes in the far-UV CD spectra exhibit a damage of the protein with a decrease of secondary structure. This is ascribed to the conjugation between protein residues and imidacloprid in the binding patch, which dwindles the stability of the biomacromolecule and finally transforms in the protein function.[43] There is explicit evidence that toxic expression evoked by imidacloprid may be associated with the improved production of reactive oxygen species (ROS), which give a good elucidation for the damage of biomacromolecules such as proteins, lipids, and nucleic acids. Duzguner and Erdogan[17] carried out an in vivo experiment to examine the acute oxidant and inflammatory effects of imidacloprid on the mammalian central nervous system and liver in 10 week old female Wistar rats. They discovered that imidacloprid exposure for 2 h notably enhance nitric oxide (NO) levels, which is a free radical signaling molecule in the nervous system of a large classification of animals and humans, in plasma, brain, and liver, and modified antioxidant activity compared with controls. They also detected significant lipid peroxidation in liver and plasma of the rats and validated either imidacloprid upraised NO free radical or other ROS might trigger off tissue damage via oxidative stress. This phenomenon excellently agrees with a more recently outcome where sodium dodecyl sulfate polyacrylamide gel electrophoresis was exploited for the investigation of human serum albumin−phorate complex.[43] However, the damage of protein does not connote a whole unfolding but adjustments on the conformation. As a matter of fact, the strong signal at 208 nm represents the presence of a heavy proportion of α helix in protein, which is still able to tie imidacloprid. Furthermore, the conformational changes of proteins upon imidacloprid complexation by far-UV CD verify the upshot of time-resolved fluorescence data and also in accordance with the induction proposed by Mikhailopulo et al.[44]

As set forth, the bioavailability of a ligand to a target tissue is influenced by its binding affinity to protein, and the reversible protein−ligand adduct play the primary role of a reservoir making free ligand usable when the concentration of the unbound ligand reduces. The unbound concentration of the ligand, thereby the biological activity, hinges on the quantity of ligand bound to protein.[45] Fluorescence combined with molecular modeling show that the imidacloprid binding site is near Trp-62 and Trp-63 residues of lysozyme and it was located at subdomain IIA of albumin. The principal driving forces between these two model proteins and imidacloprid are hydrogen bond, hydrophobic, and $\pi-\pi$ interactions, but the affinity of albumin with imidacloprid is much greater than that of lysozyme. We hold the opinion that the affinity differences between the conjugation of imidacloprid to these two proteins

originate from disparities in the three-dimensional structure. Both proteins used in this task are globular and have dissimilar sizes and amino acid sequences, that is, 14.6 kDa and 129 amino acids for lysozyme and 66.5 kDa and 585 amino acids for albumin.[26,27] Although the global structure is similar, there are great discrepancies that are pivotal to the disparate binding affinities. Subdomain IIA of albumin is a large cavity, which is related to the predominant vector function of this protein, and it could admit the accommodation of a ligand with huge size.[46,47] Additionally, it has been announced that histidine (His) is a weighty binding residue, but interactions occur with arginine (Arg) and phenylalanine (Phe) side chains. The remarkable thing is that Phe side chains are frequently buried within most of protein structure, and they are not useable as binding sites; nevertheless, Arg could fortify the association between the ligand and the peptide chain through forming an additory site of complexation but does not by itself take shape as an independent forceful binding site.[48] In the presented case, imidacloprid engenders three hydrogen bonds with the Arg-222 residue in albumin, and notable hydrophobic and $\pi-\pi$ interactions also existed between them (Phe-211 and His-242). In addition, the pyridine ring of imidacloprid was located between the benzene rings of subdomain's Phe-211 and Trp-214 residues, generating the π force similar to the "sandwich", which greatly improved the binding ability of imidacloprid and albumin. Relative to lysozyme, it is folded in two domains, and both domains are functional for the active site cleft that is formed between them.[49] The pocket established by these two domains is small, and there are no Phe, Arg, or His residues in the small cavity. In addition, the distance between imidacloprid and the subdomain IIA of albumin is much closer than the one of imidacloprid and lysozyme's hydrophobic region and therefore leads to a more powerful hydrophobic interaction in the former. This has great impact on the stable conformation of imidacloprid in the protein binding domain, and the strengthened interaction between model protein and imidacloprid. The above analyses could clarify the high affinity of imidacloprid for albumin with respect to that of lysozyme.

As well, the intrinsic strength of circulating imidacloprid conjugates for protein (especially albumin) may be much weaker than that of other intense protein−ligand adducts with affinity ranging from 10^6 to 10^8 M^{-1}, but the physiological concentration of albumin is most likely large enough (~640 μM) to let imidacloprid large-scale binding.[50] Albumin binding could effectively lengthen the in vivo half-life of imidacloprid, and the concentration of imidacloprid commonly accumulated in liver, kidney, brain, and plasma, which is in reasonable conformity with the histopathological evaluations in female rats (*Rattus norvegicus* Wistar strain) depicted elsewhere.[51] This event exerts considerable effect on toxicokinetics of the pesticide and eventually on its toxicological activity. Brunet et al.[8] conducted a human intestinal absorption of imidacloprid with the Caco-2 cell line to assess the imidacloprid bioavailability. The data convincingly suggested that imidacloprid could be highly absorbed in vivo, and the protein vector is embraced in imidacloprid uptake, in agreement with our above conjecture. The high efficiency of imidacloprid absorption and the metabolism by human cytochrome P450 enzymes in the human body could yield more toxicity than the parent compound for human health.[52] For example, a metabolite of imidacloprid, 2-imidazolidone, was evinced to elicit tumors in combination with nitrates and initiate genetic damage. It is noteworthy that long-term exposure (domestic, environmental, and occupational) to imidacloprid has been suspected to be higher toxicity than acute exposure; this consequence is unmistakably examined in a very recently study by Harris et al.[2] As already revealed by Žabar et al.,[3] 6-chloronicotinic acid, which is an end degradation product of imidacloprid under natural conditions, was confirmed in soil, vegetables, and fruits, and it can bind to protein with a greater affinity than imidacloprid.[44] It is also known that 6-chloronicotinic acid is highly soluble in water, and for that reason, it may leach from the terrestrial ecosystem toward different water bodies and ultimately enter the food chain.[53] These metabolites such as 2-imidazolidone and 6-chloronicotinic acid may be a significant contributing factor in the entire toxicology of imidacloprid.[54] By taking the above discussion into consideration, human tissues are exposed to imidacloprid through the blood, which is the important path by which toxic imidacloprid can arrive at tissues and their cells.[14,16] Comprehension of the physiologically related conjugates is therefore indispensable to the planning of important in vivo studies of imidacloprid toxicity.

The current tale lucidly narrates an integrated experimental and theoretical method of the conjugation of the highest selling neonicotinoid insecticide imidacloprid with two model proteins, lysozyme and albumin, under physiological conditions. The far-UV CD data affirm that the protein spatial structure little perturbed upon complexation with imidacloprid, with a loss of α helix following an increase in β sheet, turn, and random coil, symbolizing protein structural destabilization. Steady-state and time-resolved fluorescence certify that the quenching of lysozyme was resulted from a static type mechanism, while combined static and dynamic mechanism existed for albumin Trp fluorescence. According to molecular modeling, we can prove the imidacloprid binding site is near the Trp-62 and Trp-63 residues on lysozyme, and it was situated within subdomain IIA on albumin. Although the dominant acting forces between model protein and imidacloprid are hydrogen bond, hydrophobic, and $\pi-\pi$ interactions, the affinity of imidacloprid with albumin is superior, compared with lysozyme, which are related to the three-dimensional structure of the protein. The picked data herein may be relevant to the toxicological pattern of this extensively applied neonicotinoid insecticide imidacloprid, as the toxicology of agrochemical is, most likely, adjusted by cellular dispersion bound to abundant plasma proteins. It should also lend significant insight into these two model proteins with *moderately* toxic neonicotinoid insecticides, because the characterization and appraisal of the physiological pesticide conjugates are vital prerequisites to a grasp of the action of pernicious pesticides in human health.

AUTHOR INFORMATION

Corresponding Author

*Phone/fax: +86-10-62734676; e-mail: sunying@cau.edu.cn.

Funding

This work was executed under the auspices of the National Natural Science Foundation of China (no. 31171693).

Notes

The authors declare no competing financial interest.

ACKNOWLEDGMENTS

We are particularly indebted to Professor Ulrich Kragh-Hansen of the Department of Medical Biochemistry, University of Aarhus, for the valuable gift of his doctoral dissertation. We are

very grateful to Miss Wei Liu for her salutary contribution in language refinement and manuscript melioration. We thank Dr. Xiu-Nan Li of the Institute of Process Engineering, Chinese Academy of Sciences, for his skillful technical assistance with CD data collection. Thanks also go to the reviewers of this paper for their insightful comments.

■ ABBREVIATIONS USED

Ala, alanine; Arg, arginine; Asn, asparagine; His, histidine; Ile, isoleucine; Leu, leucine; Phe, phenylalanine; Trp, tryptophan; Val, valine; DNA, DNA; NO, nitric oxide; ROS, reactive oxygen species; Tris, tris(hydroxymethyl)aminomethane; CD, circular dichroism; IRF, instrument response function; ANOVA, analysis of variance; *R*, correlation coefficient

■ REFERENCES

(1) Ragas, A. M. J.; Oldenkamp, R.; Preeker, N. L.; Wernicke, J.; Schlink, U. Cumulative risk assessment of chemical exposures in urban environments. *Environ. Int.* **2011**, *37*, 872−881.

(2) Harris, S. A.; Villeneuve, P. J.; Crawley, C. D.; Mays, J. E.; Yeary, R. A.; Hurto, K. A.; Meeker, J. D. National study of exposure to pesticides among professional applicators: An investigation based on urinary biomarkers. *J. Agric. Food Chem.* **2010**, *58*, 10253−10261.

(3) Žabar, R.; Dolenc, D.; Jerman, T.; Franko, M.; Trebše, P. Photolytic and photocatalytic degradation of 6-chloronicotinic acid. *Chemosphere* **2011**, *85*, 861−868.

(4) Erdmanis, L.; O'Reilly, A. O.; Williamson, M. S.; Field, L. M.; Turberg, A.; Wallace, B. A. Association of neonicotinoid insensitivity with a conserved residue in the loop D binding region of the tick nicotinic acetylcholine receptor. *Biochemistry* **2012**, *51*, 4627−4629.

(5) Tomizawa, M.; Casida, J. E. Neonicotinoid insecticides: Highlights of a symposium on strategic molecular designs. *J. Agric. Food Chem.* **2011**, *59*, 2883−2886.

(6) Malato, S.; Caceres, J.; Agüera, A.; Mezcua, M.; Hernando, D.; Vial, J.; Fernández-Alba, A. R. Degradation of imidacloprid in water by photo-Fenton and TiO_2 photocatalysis at a solar pilot plant: A comparative study. *Environ. Sci. Technol.* **2001**, *35*, 4359−4366.

(7) Nougadère, A.; Reninger, J.-C.; Volatier, J.-L.; Leblanc, J.-C. Chronic dietary risk characterization for pesticide residues: A ranking and scoring method integrating agricultural uses and food contamination data. *Food Chem. Toxicol.* **2011**, *49*, 1484−1510.

(8) Brunet, J.-L.; Maresca, M.; Fantini, J.; Belzunces, L. P. Human intestinal absorption of imidacloprid with Caco-2 cells as enterocyte model. *Toxicol. Appl. Pharmacol.* **2004**, *194*, 1−9.

(9) Flores-Céspedes, F.; Figueredo-Flores, C. I.; Daza-Fernández, I.; Vidal-Peña, F.; Villafranca-Sánchez, M.; Fernández-Pérez, M. Preparation and characterization of imidacloprid lignin-polyethylene glycol matrices coated with ethylcellulose. *J. Agric. Food Chem.* **2012**, *60*, 1042−1051.

(10) Jugan, M.-L.; Levi, Y.; Blondeau, J.-P. Endocrine disruptors and thyroid hormone physiology. *Biochem. Pharmacol.* **2010**, *79*, 939−947.

(11) http://www.regulations.gov/#!documentDetail;D=EPA-HQ-OPP-2012-0204-0003 (accessed May 23, 2012).

(12) European Food Safety Authority. http://www.efsa.europa.eu/en/efsajournal/pub/1589.htm (accessed April 23, 2010).

(13) Health Canada. http://www.hc-sc.gc.ca/cps-spc/pubs/pest/_decisions/emrl2011-51/index-eng.php (accessed September 21, 2011).

(14) Feng, S. L.; Kong, Z. M.; Wang, X. M.; Peng, P. G.; Zeng, E. Y. Assessing the genotoxicity of imidacloprid and RH-5849 in human peripheral blood lymphocytes in vitro with comet assay and cytogenetic tests. *Ecotoxicol. Environ. Saf.* **2005**, *61*, 239−246.

(15) Demsia, G.; Vlastos, D.; Goumenou, M.; Matthopoulos, D. P. Assessment of the genotoxicity of imidacloprid and metalaxyl in cultured human lymphocytes and rat bone-marrow. *Mutat. Res., Genet. Toxicol. Environ. Mutagen.* **2007**, *634*, 32−39.

(16) Costa, C.; Silvari, V.; Melchini, A.; Catania, S.; Heffron, J. J.; Trovato, A.; de Pasquale, R. Genotoxicity of imidacloprid in relation to metabolic activation and composition of the commercial product. *Mutat. Res., Genet. Toxicol. Environ. Mutagen.* **2009**, *672*, 40−44.

(17) Duzguner, V.; Erdogan, S. Acute oxidant and inflammatory effects of imidacloprid on the mammalian central nervous system and liver in rats. *Pestic. Biochem. Physiol.* **2010**, *97*, 13−18.

(18) El-Gendy, K. S.; Aly, N. M.; Mahmoud, F. H.; Kenawy, A.; El-Sebae, A. K. H. The role of vitamin C as antioxidant in protection of oxidative stress induced by imidacloprid. *Food Chem. Toxicol.* **2010**, *48*, 215−221.

(19) Kapoor, U.; Srivastava, M. K.; Srivastava, L. P. Toxicological impact of technical imidacloprid on ovarian morphology, hormones and antioxidant enzymes in female rats. *Food Chem. Toxicol.* **2011**, *49*, 3086−3089.

(20) Park, Y.; Kim, Y.; Kim, J.; Yoon, K. S.; Clark, J.; Lee, J.; Park, Y. Imidacloprid, a neonicotinoid insecticide, potentiates adipogenesis in 3T3-L1 adipocytes. *J. Agric. Food Chem.* **2013**, *61*, 255−259.

(21) Gawade, L.; Dadarkar, S. S.; Husain, R.; Gatne, M. A detailed study of developmental immunotoxicity of imidacloprid in Wistar rats. *Food Chem. Toxicol.* **2013**, *51*, 61−70.

(22) Proença, P.; Teixeira, H.; Castanheira, F.; Pinheiro, J.; Monsanto, P. V.; Marques, E. P.; Vieira, D. N. Two fatal intoxication cases with imidacloprid: LC/MS analysis. *Forensic Sci. Int.* **2005**, *153*, 75−80.

(23) Huang, N.-C.; Lin, S.-L.; Chou, C.-H.; Hung, Y.-M.; Chung, H.-M.; Huang, S.-T. Fatal ventricular fibrillation in a patient with acute imidacloprid poisoning. *Am. J. Emerg. Med.* **2006**, *24*, 883−885.

(24) Shadnia, S.; Moghaddam, H. H. Fatal intoxication with imidacloprid insecticide. *Am. J. Emerg. Med.* **2008**, *26*, 634.e1−634.e4.

(25) Abou-Zied, O. K. Revealing the ionization ability of binding site I of human serum albumin using 2-(2′-hydroxyphenyl)benzoxazole as a pH sensitive probe. *Phys. Chem. Chem. Phys.* **2012**, *14*, 2832−2839.

(26) Blake, C. C. F.; Koenig, D. F.; Mair, G. A.; North, A. C. T.; Phillips, D. C.; Sarma, V. R. Structure of hen egg-white lysozyme: A three-dimensional Fourier synthesis at 2 Å resolution. *Nature* **1965**, *206*, 757−761.

(27) Carter, D. C.; He, X.-M.; Munson, S. H.; Twigg, P. D.; Gernert, K. M.; Broom, M. B.; Miller, T. Y. Three-dimensional structure of human serum albumin. *Science* **1989**, *244*, 1195−1198.

(28) Seiber, J. N.; Kleinschmidt, L. A. Contributions of pesticide residue chemistry to improving food and environmental safety: Past and present accomplishments and future challenges. *J. Agric. Food Chem.* **2011**, *59*, 7536−7543.

(29) Mostafalou, S.; Abdollahi, M. Pesticides and human chronic diseases: Evidences, mechanisms, and perspectives. *Toxicol. Appl. Pharmacol.* **2013**, *268*, 157−177.

(30) Lowry, O. H.; Rosebrough, N. J.; Farr, A. L.; Randall, R. J. Protein measurement with the Folin phenol reagent. *J. Biol. Chem.* **1951**, *193*, 265−275.

(31) Greenfield, N. J. Using circular dichroism spectra to estimate protein secondary structure. *Nat. Protoc.* **2006**, *1*, 2876−2890.

(32) Lakowicz, J. R. *Principles of Fluorescence Spectroscopy*, 3rd ed.; Springer: New York, 2006; pp 97−330.

(33) Endo, S.; Bauerfeind, J.; Goss, K.-U. Partitioning of neutral organic compounds to structural proteins. *Environ. Sci. Technol.* **2012**, *46*, 12697−12703.

(34) Dubeau, S.; Bourassa, P.; Thomas, T. J.; Tajmir-Riahi, H. A. Biogenic and synthetic polyamines bind bovine serum albumin. *Biomacromolecules* **2010**, *11*, 1507−1515.

(35) Mahato, M.; Pal, P.; Kamilya, T.; Sarkar, R.; Chaudhuri, A.; Talapatra, G. B. Hemoglobin-silver interaction and bioconjugate formation: A spectroscopic study. *J. Phys. Chem. B* **2010**, *114*, 7062−7070.

(36) Bourassa, P.; Tajmir-Riahi, H. A. Locating the binding sites of folic acid with milk α- and β-caseins. *J. Phys. Chem. B* **2012**, *116*, 513−519.

(37) Jha, N. S.; Kishore, N. Binding of streptomycin with bovine serum albumin: Energetics and conformational aspects. *Thermochim. Acta* **2009**, *482*, 21−29.
(38) Wang, Y.-Q.; Tang, B.-P.; Zhang, H.-M.; Zhou, Q.-H.; Zhang, G.-C. Studies on the interaction between imidacloprid and human serum albumin: Spectroscopic approach. *J. Photochem. Photobiol., B* **2009**, *94*, 183−190.
(39) World Health Organization. The WHO Recommended Classification of Pesticides by Hazard and Guidelines to Classification 2009. http://www.who.int/ipcs/publications/pesticides_hazard_2009.pdf (accessed 2010).
(40) Hodges, L.; Bell, J.; Adam, K. *Petition for a Three-Year Extension of Exclusive Use Data Protection for Spirotetramat*, Report no. US0222; U.S. Environmental Protection Agency Office of Pesticide Programs: Washington, DC, 2012.
(41) Tinoco, A. D.; Eames, E. V.; Valentine, A. M. Reconsideration of serum Ti(IV) transport: Albumin and transferrin trafficking of Ti(IV) and its complexes. *J. Am. Chem. Soc.* **2008**, *130*, 2262−2270.
(42) Cheema, M. A.; Taboada, P.; Barbosa, S.; Juárez, J.; Gutiérrez-Pichel, M.; Siddiq, M.; Mosquera, V. Human serum albumin unfolding pathway upon drug binding: A thermodynamic and spectroscopic description. *J. Chem. Thermodyn.* **2009**, *41*, 439−447.
(43) Saquib, Q.; Al-Khedhairy, A. A.; Siddiqui, M. A.; Roy, A. S.; Dasgupta, S.; Musarrat, J. Preferential binding of insecticide phorate with sub-domain IIA of human serum albumin induces protein damage and its toxicological significance. *Food Chem. Toxicol.* **2011**, *49*, 1787−1795.
(44) Mikhailopulo, K. I.; Serchenya, T. S.; Kiseleva, E. P.; Chernov, Y. G.; Tsvetkova, T. M.; Kovganko, N. V.; Sviridov, O. V. Interaction of molecules of the neonicotinoid imidacloprid and its structural analogs with human serum albumin. *J. Appl. Spectrosc.* **2008**, *75*, 857−863.
(45) Rosengren, A. M.; Karlsson, B. C. G.; Nicholls, I. A. Monitoring the distribution of warfarin in blood plasma. *ACS Med. Chem. Lett.* **2012**, *3*, 650−652.
(46) Kragh-Hansen, U. Structure and ligand binding properties of human serum albumin. Ph.D. Thesis, University of Aarhus, Aarhus, Denmark, 1989.
(47) Kragh-Hansen, U. Evidence for a large and flexible region of human serum albumin possessing high affinity binding sites for salicylate, warfarin, and other ligands. *Mol. Pharmacol.* **1988**, *34*, 160−171.
(48) de Wolf, F. A.; Brett, G. M. Ligand-binding proteins: Their potential for application in systems for controlled delivery and uptake of ligands. *Pharmacol. Rev.* **2000**, *52*, 207−236.
(49) Ford, S. J.; Cooper, A.; Hecht, L.; Wilson, G.; Barron, L. D. Vibrational Raman optical activity of lysozyme: Hydrogen-deuterium exchange, unfolding and ligand binding. *J. Chem. Soc., Faraday Trans.* **1995**, *91*, 2087−2093.
(50) Quinlan, G. J.; Martin, G. S.; Evans, T. W. Albumin: Biochemical properties and therapeutic potential. *Hepatology* **2005**, *41*, 1211−1219.
(51) Bhardwaj, S.; Srivastava, M. K.; Kapoor, U.; Srivastava, L. P. A 90 days oral toxicity of imidacloprid in female rats: Morphological, biochemical and histopathological evaluations. *Food Chem. Toxicol.* **2010**, *48*, 1185−1190.
(52) Schulz-Jander, D.; Casida, J. E. Imidacloprid insecticide metabolism: Human cytochrome P450 isozymes differ in selectivity for imidazolidine oxidation versus nitroimine reduction. *Toxicol. Lett.* **2002**, *132*, 65−70.
(53) Dell'Arciprete, M. L.; Santos-Juanes, L.; Sanz, A. A.; Vicente, R.; Amat, A. M.; Furlong, J. P.; Mártire, D. O.; Gonzalez, M. C. Reactivity of hydroxyl radicals with neonicotinoid insecticides: Mechanism and changes in toxicity. *Photochem. Photobiol. Sci.* **2009**, *8*, 1016−1023.
(54) Chao, S. L.; Casida, J. E. Interaction of imidacloprid metabolites and analogs with the nicotinic acetylcholine receptor of mouse brain in relation to toxicity. *Pestic. Biochem. Physiol.* **1997**, *58*, 77−88.